Potential characterization of free-space-wave drop demultiplexer using cavity-resonator-integrated grating input/output coupler

Kenji Kintaka,[1,*] Katsuya Shimizu,[2] Yuki Kita,[2] Satoshi Kawanami,[2] Junichi Inoue,[2] Shogo Ura,[2] and Junji Nishii[3]

[1]*Photonics Research Institute, National Institute of Advanced Industrial Science and Technology, Central 2, 1-1-1 Umezono, Tsukuba, Ibaraki 305-8568, Japan*
[2]*Department of Electronics, Kyoto Institute of Technology, Matugasaki, Sakyo-ku, Kyoto 606-8585, Japan*
[3]*Research Institute for Electronic Science, Hokkaido University, Kita 21 Nishi 10, Kita-ku, Sapporo 001-0021, Japan*
**kintaka.kenji@aist.go.jp*

Abstract: A prototype free-space-wave drop demultiplexer consisting of a cavity-resonator-integrated grating input/output coupler (CRIGIC) and a different-guided-mode-coupling distributed Bragg reflector (DGM-DBR) was designed for constructing a high-density wavelength-division-multiplexing intra-board chip-to-chip optical interconnection. The CRIGIC consists of one grating coupler and two DBRs, and can vertically couple a guided wave and a free-space wave with high efficiency. A two-channel drop demultiplexer operating at around 850-nm wavelength with 5-nm channel spacing in wavelength was fabricated in a thin-film SiO_2-based waveguide. The device performance was predicted theoretically, characterized experimentally, and discussed.

OCIS codes: (130.0130) Integrated optics; (230.3120) Integrated optics devices; (230.1480) Bragg reflectors; (230.1950) Diffraction gratings; (230.7370) Waveguides; (130.7408) Wavelength filtering devices.

References and links

1. N. Savage, "Linking with light [high-speed optical interconnects]," IEEE Spectrum **39**(8), 32–36 (2002).
2. A. F. Benner, M. Ignatowski, J. A. Kash, D. M. Kuchta, and M. B. Ritter, "Exploitation of optical interconnects in future sever architectures," IBM J. Res. Develop. **49**(4), 755–775 (2005).
3. L. Schares, J. A. Kash, F. E. Doany, C. L. Schow, C. Schuster, D. M. Kuchta, P. K. Pepeljugoski, J. M. Trewhella, C. W. Baks, R. A. John, L. Shan, Y. H. Kwark, R. A. Budd, P. Chiniwalla, F. R. Libsch, J. Rosner, C. K. Tsang, C. S. Patel, J. D. Schaub, R. Dangel, F. Horst, B. J. Offrein, D. Kucharski, D. Guckenberger, S. Hegde, H. Nyikal, C.-K. Lin, A. Tandon, G. R. Trott, M. Nystrom, D. P. Bour, M. R. T. Tan, and D. W. Dolfi, "Terabus: terabit/second-class card-level optical interconnect technologies," IEEE J. Sel. Top. Quantum Electron. **12**(5), 1032–1044 (2006).
4. F. R. Libsch, R. Budd, P. Chiniwalla, P. C. D. Hobbs, M. Mastro, J. L. Sanford, and J. Xu, "MCM LGA package with optical I/O passively aligned to dual layer polymer waveguide in PCB," in *Proceedings of IEEE 56th Electronics Components and Technology Conference* (Institute of Electrical and Electronics Engineers, New York, 2006), pp. 1693–1699.
5. M. Shishikura, Y. Matsuoka, T. Ban, T. Shibara, and A. Takahashi, "A high-coupling efficiency multilayer optical printed wiring board with a cube-core structure for high-density optical interconnections," in *Proceedings of IEEE 57th Electronics Components and Technology Conference* (Institute of Electrical and Electronics Engineers, New York, 2007), pp. 1275–1280.
6. S.-H. Hwang, M. H. Cho, S.-K. Kang, T.-W. Lee, H.-H. Park, and B. S. Rho, "Two-dimensional optical interconnection based on two-layered optical printed circuit board," IEEE Photon. Technol. Lett. **19**(6), 411–413 (2007).
7. J.-S. Kim, and J.-J. Kim, "Stacked polymeric multimode waveguide arrays for two-dimensional optical interconnects," J. Lightwave Technol. **22**(3), 840–844 (2004).
8. N. Hendrickx, J. Van Erps, G. Van Steenberge, H. Thienpont, and P. Van Daele, "Tolerance Analysis for Multilayer Optical Interconnections Integrated on a Printed Circuit Board," J. Lightwave Technol. **25**(9), 2395–2401 (2007).
9. S. Ura, "Selective guided mode coupling via bridging mode by integrated gratings for Intraboard optical interconnects," Proc. SPIE **4652**, 86–96 (2002).
10. K. Kintaka, J. Nishii, K. Shinoda, and S. Ura, "WDM signal transmission in a thin-film waveguide for optical interconnection," IEEE Photon. Technol. Lett. **18**(21), 2299–2301 (2006).

#132794 - $15.00 USD Received 2 Aug 2010; revised 2 Nov 2010; accepted 5 Nov 2010; published 17 Nov 2010

11. K. Kintaka, J. Nishii, S. Murata, and S. Ura, "Eight-channel WDM Intraboard optical interconnect device by integration of add/drop multiplexers in thin-film waveguide," J. Lightwave Technol. **28**(9), 1398–1403 (2010).
12. C. Gunn, "CMOS photonics for high-speed interconnects," IEEE Micro **26**(2), 58–66 (2006).
13. D. Taillaert, W. Bogaerts, P. Bienstman, T. F. Krauss, P. Van Daele, I. Moerman, S. Verstuyft, K. De Mesel, and R. Baets, "An out-of-plane grating coupler for efficient butt-coupling between compact planar waveguides and single-mode fibers," IEEE J. Quantum Electron. **38**(7), 949–955 (2002).
14. G. Roelkens, D. Vermeulen, F. Van Laere, S. Selvaraja, S. Scheerlinck, D. Taillaert, W. Bogaerts, P. Dumon, D. Van Thourhout, and R. Baets, "Bridging the gap between nanophotonic waveguide circuits and single mode optical fibers using diffractive grating structures," J. Nanosci. Nanotechnol. **10**(3), 1551–1562 (2010).
15. X. Chen, C. Li, and H. K. Tsang, "Fabrication-tolerant waveguide chirped grating coupler for coupling to a perfectly vertical optical fiber," IEEE Photon. Technol. Lett. **20**(23), 1914–1916 (2008).
16. S. Ura, S. Murata, Y. Awatsuji, and K. Kintaka, "Design of resonance grating coupler," Opt. Express **16**(16), 12207–12213 (2008).
17. K. Kintaka, Y. Kita, K. Shimizu, H. Matsuoka, S. Ura, and J. Nishii, "Cavity-resonator-integrated grating input/output coupler for high-efficiency vertical coupling with a small aperture," Opt. Lett. **35**(12), 1989–1991 (2010).
18. S. Ura, K. Shimizu, Y. Kita, K. Kintaka, J. Inoue, and Y. Awatsuji, "Cavity-resonator-integrated grating input/output couplers for WDM optical-interconnect system in package," in *Proceedings of IEEE 60th Electronic Components and Technology Conference* (Institute of Electrical and Electronics Engineers, New York, 2010), pp. 263–268.

1. Introduction

Intra-board chip-to-chip interconnection with ultra-broadband bandwidth over terabits-per-second and high wiring density is required for near-future high-performance computing systems, and optical interconnection is one of the promising candidates to enable such the signal transmission [1,2]. Two-dimensional (2D) parallel signal transmission from a vertical-cavity surface emitting laser (VCSEL) array in a transmitter chip to a photodiode (PD) array in a receiver chip is one of the most attractive techniques, taking into account that a bandwidth of a single channel is limited by the direct modulation speed of VCSELs and/or the electronic circuits. Several optical interconnect configurations for realization of such the 2D signal transmission have been reported so far using a multimode waveguide array as optical paths [3–8]. On the other hand, we have proposed and investigated another approach using wavelength-division multiplexing (WDM) technique for such the 2D signal transmission with high wiring density [9–11]. Free-space-wave add/drop multiplexers (ADMs) are utilized in the proposed technique for coupling between WDM guided waves and free-space waves. The ADM consists of a grating coupler (GC) and a different-guided-mode-coupling distributed Bragg reflector (DGM-DBR) integrated in a thin-film double-core-structure waveguide. Two-channel WDM signal transmission [10] and eight-channel ADM [11] have been demonstrated experimentally by using the fabricated device so far. However, the channel width was a few hundreds micrometers, which was determined by the aperture size, i.e. the coupling length of GC, and did not directly match the beam size of several micrometers from a single-mode VCSEL. In order to realize higher wiring density, GC should have an aperture size of several micrometers.

The aperture size of GC is determined by the radiation decay factor of GC in order to realize high efficiency. The radiation decay factor depends on and is limited by the modulation depth of refractive index in the grating structure. The modulation depth required for high-efficiency GC with several-micrometer aperture can be obtained in semiconductor waveguides due to their large refractive indices [12–15]. On the other hand, it is difficult to obtain such a short GC in a dielectric waveguide because of its relatively low refractive index. Recently, we have proposed and investigated a new-type GC, namely cavity-resonator-integrated grating input/output coupler (CRIGIC), in order to realize high-efficiency vertical coupling with a small aperture in a dielectric waveguide [16,17].

This time, we tried to integrate CRIGIC and DGM-DBR in order to construct an ADM. The integration of CRIGICs and DGM-DBRs will enable to provide 3200 transmission channels within 10-mm width by combination of 8-channel WDM and 400 waveguide channels with 25 μm pitch. The number of transmission channels is six times as large as that of the previous configuration using GCs and DGM-DBRs [9]. The maximum transmission bandwidth of 16 Tb/s/cm is expected in the proposed interconnect configuration, provided a

#132794 - $15.00 USD Received 2 Aug 2010; revised 2 Nov 2010; accepted 5 Nov 2010; published 17 Nov 2010

bit rate for a signal channel is 10 Gb/s. This value matches the one required in ten years according to the International Technology Roadmap for Semiconductors, but it is difficult to realize by other interconnect configurations. We designed and fabricated a prototype two-channel drop demultiplexer in a SiO_2-based single-core waveguide operating at around 850-nm wavelength with 5-nm channel spacing in wavelength, and characterized its performance and potential to clarify the feasibility of the ADM using CRIGIC for the first time. Besides an expected miniaturization of the aperture size, it was theoretically predicted and experimentally confirmed that the crosstalk noise was greatly improved in comparison with a device using GC instead of CRIGIC, which was attributed to the wavelength dispersion of CRIGIC. However, we also observed an unpredicted and undesirable diffraction by DBRs in CRIGIC, which should be avoided in practical devices. In this paper, we report and discuss the prototype design and the obtained experimental results of the two-channel drop demultiplexer.

2. Basic configuration of free-space-wave add/drop multiplexer

Basic cross-sectional configuration of WDM optical interconnection using the proposed ADMs with CRIGICs is illustrated in Fig. 1. Only two WDM signal channels are shown in the figure for simplicity. Optoelectronic interposers integrating an array of single-mode linearly polarized VCSELs and a PD array are surface-mounted with LSI chips on a waveguide. CRIGICs and DGM-DBRs are integrated in the waveguide, and an add multiplexer or a drop demultiplexer for one channel is constructed by a pair of CRIGIC and DGM-DBR. The fundamental and the first-order TE guided modes are utilized as a signal transmission and an input/output waves, respectively. A free-space wave at wavelength λ_1 from a VCSEL is coupled by $CRIGIC_{1i}$ to TE_1 guided wave propagating to left-hand side. The TE_1 guided wave is contra-directionally coupled by $DGM\text{-}DBR_{1i}$ to TE_0 guided wave. The TE_0 guided wave passes through $CRIGIC_{1i}$, and also passes through the other pair of $CRIGIC_{2i}$ and $DGM\text{-}DBR_{2i}$ for the other wavelength channel in the transmitter side. In the receiver side, the propagated TE_0 guided wave passes through $CRIGIC_{1o}$ and is contra-directionally coupled by $DGM\text{-}DBR_{1o}$ to TE_1 guided wave. The TE_1 guided wave is vertically coupled out by $CRIGIC_{1o}$ to a free-space wave, and detected by a PD. In the same way, a free-space wave at wavelength λ_2 from the other VCSEL is transmitted by $CRIGIC_{2i}$, $DGM\text{-}DBR_{2i}$, $DGM\text{-}DBR_{2o}$, and $CRIGIC_{2o}$, and is detected by the other PD.

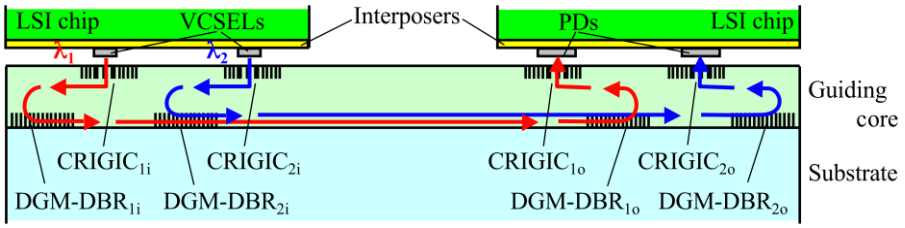

Fig. 1. Cross-sectional schematic view of WDM optical interconnection using free-space-wave ADMs with CRIGICs.

3. Design of drop demultiplexer

In order to confirm the operation principle of the new-combination of CRIGIC and DGM-DBR, a prototype two-channel drop demultiplexer was designed for operating at around 850-nm wavelength. The cross-sectional structure and refractive index profile of the designed waveguide are illustrated in Fig. 2. The waveguide consists of a 0.25-μm-thick electron beam (EB) resist grating layer with refractive index of 1.55, a 1.24-μm-thick Ge-SiO_2 core layer with refractive index of 1.54, and a 15-nm-thick Si-N grating layer with refractive index of 2.01 on a SiO_2 substrate with refractive index of 1.452. CRIGIC and DGM-DBR patterns are formed in the EB resist and Si-N layers, respectively.

#132794 - $15.00 USD Received 2 Aug 2010; revised 2 Nov 2010; accepted 5 Nov 2010; published 17 Nov 2010

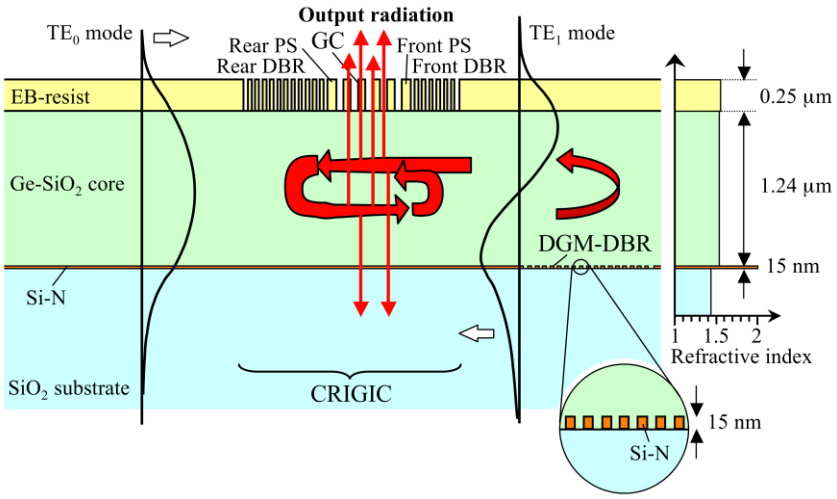

Fig. 2. Cross-sectional structure and refractive index profile of the designed waveguide device.

The calculated electric-field profile of TE_0 and TE_1 modes are also shown in Fig. 2. The effective refractive indices of TE_0 and TE_1 modes at DGM-DBR area were calculated to be 1.525 and 1.481, respectively. The grating period of the DGM-DBR was 281.1 nm for 845-nm wavelength. The coupling coefficient of DGM-DBR between TE_0 and TE_1 guided waves was calculated to be 8.9 mm^{-1} by the coupled mode analysis. The coupling efficiency and full-width at half maximum (FWHM) of wavelength selectivity of the DGM-DBR were predicted to be 98% and 1.7 nm, respectively, with the coupling length of 300 μm.

CRIGIC consists of one vertical-coupling GC integrated between two DBRs with phase-shifting spaces (PSs). The concept and design principle of CRIGIC have been described in detail previously [16,17]. Coupling characteristics of CRIGIC were estimated by the coupled mode analysis. The effective refractive indices of TE_0 and TE_1 modes at CRIGIC area were calculated to be 1.523 and 1.471, respectively. GC period, DBR period, and PS length in CRIGIC were 574.4 nm (= Λ), 287.2 nm (= Λ/2), and 215.4 nm (= 3/8·Λ), respectively, for 845-nm wavelength. The radiation decay factors of GC in CRIGIC for TE_0 and TE_1 modes were calculated to be 1.1 mm^{-1} and 4.6 mm^{-1}, respectively. The coupling coefficient of DBR in CRIGIC for TE_1 mode was calculated to be 28 mm^{-1}. The coupling length of GC in CRIGIC was chosen to be 9.8 μm (= 17Λ). The coupling lengths of the front and rear DBRs in CRIGIC were determined to be 42.5 μm (= 74Λ) and 115 μm (= 200Λ), respectively. The reflection efficiencies of the front and rear DBRs in CRIGIC for TE_1 mode were predicted to be 83% and 99.7%, respectively. Figure 3 shows the calculated wavelength dependences of output, transmission, and reflection efficiencies of CRIGIC for TE_1 mode. The maximum output efficiency was estimated to be 60%. The output efficiency was limited by a power distribution ratio to the output air radiation against all the radiation, which was calculated to be 0.61. The rest of 40% includes the substrate radiation of 38% and the transmission of 2%, and becomes to the loss. The output efficiency of CRIGIC can be enhanced by using a Au reflection layer on the substrate [17]. However, it needs the deposition of the Au and optical buffer layers as well as the careful control of the buffer layer thickness. This time, we did not use a Au reflection layer in order to avoid the unessential complexity. The output efficiency of CRIGIC was 11 times as high as that of a conventional GC with the same aperture size and the same radiation decay factor. FWHM of wavelength selectivity of the CRIGIC was predicted to be 0.9 nm.

#132794 - $15.00 USD Received 2 Aug 2010; revised 2 Nov 2010; accepted 5 Nov 2010; published 17 Nov 2010

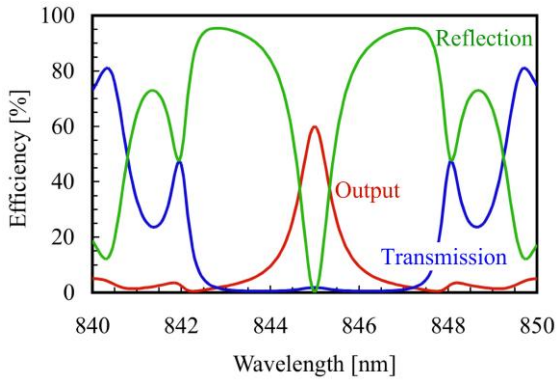

Fig. 3. Calculated wavelength dependences of output, transmission, and reflection efficiencies of the CRIGIC designed for TE_1 mode.

The device characteristics of the two-channel drop demultiplexer were predicted theoretically. The two-channel drop demultiplexer consists of two pairs of CRIGICs and DGM-DBRs. The calculated wavelength dependence of the drop demultiplexer is shown in Fig. 4(a). Operating wavelengths for channel-1 (λ_1) and channel-2 (λ_2) were set to be 847 nm and 842 nm, respectively. The maximum output efficiencies for channel-1 and channel-2 were predicted to be 59% and 57%, respectively. FWHM of wavelength selectivity for each channel was calculated to be 0.9 nm. The bandwidth of the drop demultiplexer was broad enough to transmit 10 Gb/s signals. The crosstalk noise levels for channel-1 and channel-2 at operation wavelengths were calculated to be –16 dB and –34 dB, respectively. The main cause of the crosstalk noise for channel-1 is the air radiation of TE_0 guided wave with λ_2 wavelength coupled by GC in the first CRIGIC (shown by $CRIGIC_1$ in Fig. 5). On the other hand, TE_0 guided wave with λ_1 wavelength is coupled out by the first drop demultiplexer and hardly reaches the second CRIGIC (shown by $CRIGIC_2$ in Fig. 5) so that the crosstalk noise for channel-2 is extremely small. The wavelength dependence of a two-channel drop demultiplexer using conventional GCs with 200-μm coupling length instead of CRIGICs was also estimated for comparison. The calculated result is shown in Fig. 4(b). A red curve indicated as channel-1 shows the output power from the first GC (GC_1) assigned to 847-nm wavelength channel. Since the output coupling efficiency of GC_1 has little dependence on wavelength, the forward-going TE_0 signal-transmission wave is diffracted to the air radiation with almost constant efficiency higher than 20% in this case. At around the coupling wavelength of 847 nm, the backward TE_1 input/output wave generated by the first DGM-DBR is strongly diffracted by GC_1 to the output air radiation. The other blue curve denoted channel-2 shows the output power from the second GC (GC_2) assigned to 842-nm wavelength channel. The power of TE_0 guided wave reaching GC_2 is the rest of the diffraction occurred in the first drop demultiplexer for 847 nm. Then both the wavelength-independent air-radiation power due to TE_0 diffraction and the output power at the coupling wavelength of 842 nm are about two-thirds of those for channel-1. The reason for the power drop at around 847 nm in channel-2 is that most of TE_0 guided wave is diffracted out by the first drop demultiplexer and does not reach the second drop demultiplexer. The crosstalk noise levels for channel-1 and channel-2 at operation wavelengths were calculated to be –3 dB and –21 dB, respectively. Thus, the great improvements in the output-power-level equivalence and signal-to-noise ratio are expected when a free-space-wave drop demultiplexer is constructed by using CRIGIC instead of GC.

#132794 - $15.00 USD Received 2 Aug 2010; revised 2 Nov 2010; accepted 5 Nov 2010; published 17 Nov 2010

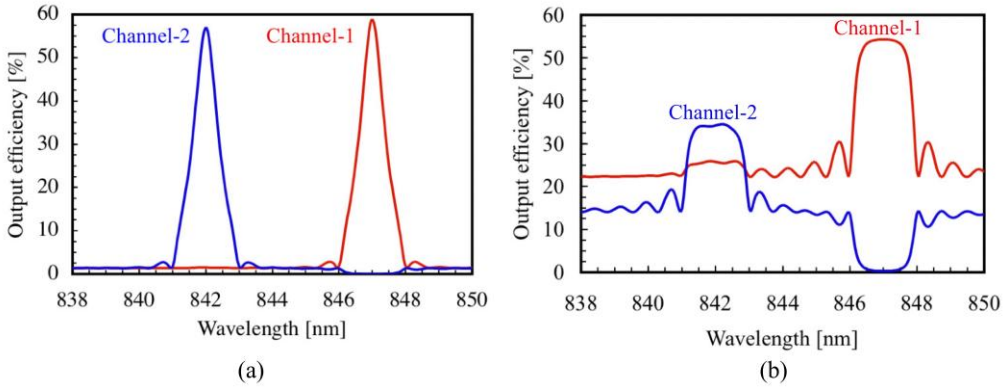

Fig. 4. Calculated wavelength dependences of two-channel drop demultiplexers using (a) CRIGICs and (b) GCs.

4. Fabrication and characterization

A schematic view of the fabricated two-channel drop demultiplexer is shown in Fig. 5. A Si-N grating layer with 15-nm thickness was deposited on a SiO_2 substrate by reactive DC sputtering. After an EB resist was spin-coated, DGM-DBR patterns of 281.76-nm and 280.08-nm grating periods with 0.3-mm coupling length were formed by EB direct writing for channel-1 and channel-2, respectively. The DGM-DBR patterns were transferred to the Si-N layer by reactive ion etching. A Ge-SiO_2 core layer with 1.24-μm thickness was deposited by plasma-enhanced chemical vapor deposition. An EB-resist grating layer with 0.25-μm thickness was spin-coated, and CRIGIC patterns with Λ of 574.90 nm and 571.54 nm were fabricated by EB direct writing and developing for channel-1 and channel-2, respectively. The two-channel drop demultiplexer with GC patterns of 0.6-μm grating period and 0.2-mm coupling length instead of CRIGIC patterns were also fabricated on the same substrate for comparison. Input GCs of 1.3-μm grating period were also formed for exciting TE_0 guided wave into the waveguide, as shown in Fig. 5. The distance between the input GC and $CRIGIC_1$ was 15 mm, and the distance between the two channels was 0.75 mm.

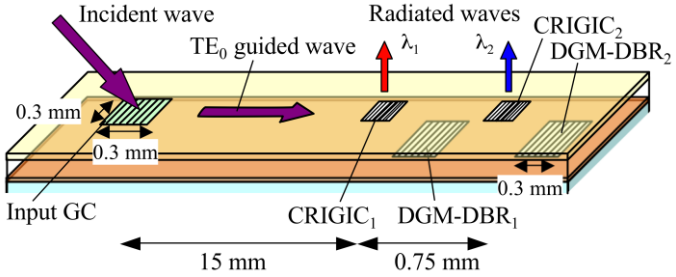

Fig. 5. Schematic view of the two-channel drop demultiplexer using CRIGICs.

A tunable laser diode was used as a light source in the device characterization, and TE_0 guided wave was excited by the input GC. Figure 6(a) shows the measured wavelength dependence of the two-channel drop demultiplexer using CRIGICs. The output efficiencies for channel-1 and channel-2 are shown by open and closed circles, respectively, in the figure. Since the absolute power of TE_0 guided wave excited by the input GC cannot be measured exactly in this experiment, the output efficiencies are presented by relative values. The maximum output efficiencies were obtained at 847.2 nm and 842.5 nm for channel-1 and channel-2, respectively. FWHM of wavelength selectivity was measured to be 0.7 nm for each channel, which was close to the predicted value of 0.9 nm. The crosstalk noise levels for channel-1 and channel-2 were measured to be −13 dB and −18 dB, respectively. The

#132794 - $15.00 USD Received 2 Aug 2010; revised 2 Nov 2010; accepted 5 Nov 2010; published 17 Nov 2010

difference between the predicted and experimental values of the crosstalk noise level for channel-2 is due to the measurement limit of about –20 dB. On the other hand, the measured wavelength dependence of the two-channel drop demultiplexer using GCs is shown in Fig. 6(b). The output efficiencies for channel-1 and channel-2 are shown by open and closed triangles, respectively. The vertical scale is equal to that of Fig. 6(a). The maximum output efficiencies for channel-1 and channel-2 were obtained at 847.2 nm and 842.0 nm, respectively. The crosstalk noise levels for channel-1 and channel-2 at operating wavelengths were measured to be –3 dB and –12 dB, respectively. Thus, the predicted great improvement in crosstalk-noise reduction was successfully demonstrated. The obtained output efficiency for channel-2 in the drop demultiplexer using CRIGICs, however, was considerably lower than the prediction. The reason for such the low output efficiency was investigated and identified as discussed in the next paragraph.

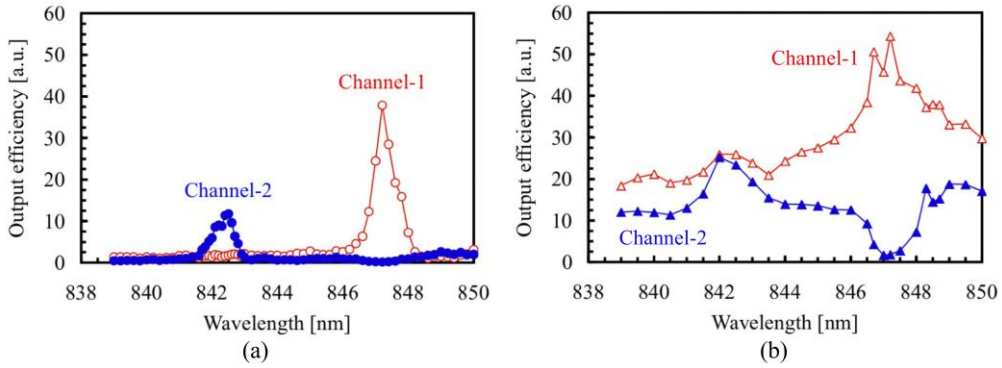

Fig. 6. Measured wavelength dependences of two-channel demultiplexers using (a) CRIGICs and (b) GCs.

A wave vector diagram of CRIGIC, which couples with TE_0 mode, is depicted in Fig. 7(a). The radii of the upper semicircle k_0 (= $2\pi/\lambda$) and the lower semicircle $k_0 n_s$ indicate wave numbers in air and in the substrate of refractive index n_s, respectively. TE_0 guided wave propagating along z-axis is denoted by an arrow $k_0 N_0$, where N_0 is the effective refractive index. The grating vectors of GC and DBR in CRIGIC are indicated by K_{GC} (= $2\pi/\Lambda$) and K_{DBR} (= $2 \cdot 2\pi/\Lambda$), respectively. Figure 7(a) indicates that the TE_0 guided wave is coupled by GC to the air radiation and the substrate radiation waves denoted by the red allows. These radiations have already been considered in the predicted wavelength dependence shown in Fig. 4(a). Waveguide DBRs are designed to couple two contra-directional guided waves, and their grating vectors are just twice of the wave vectors of guided waves. Thus, the grating vectors are normally too large to couple radiation waves. In the current case, however, utilization of two guided modes made the situation complicated. DBR in CRIGIC was designed to couple two TE_1 guided waves contra-directionally, and the wave vector of TE_1 guided wave is smaller than that of TE_0 guided wave, which causes a risk of diffraction of TE_0 guided wave to the substrate radiation. This substrate radiation is illustrated in Fig. 7(a) by an arrow k_d of which z component matches to $k_0 N_0 + K_{DBR}$. Figure 7(b) shows the calculated wavelength dependence of the two-channel drop demultiplexer using CRIGICs with consideration for such the substrate radiation losses of TE_0 guided wave caused by DBRs in CRIGICs. The recalculated wavelength dependence is in good agreement with the measurement results shown in Fig. 6(a). As a result, the main reason for the imbalance in output efficiency of the drop demultiplexer using CRIGICs can be explained by the substrate radiation from TE_0 guided wave coupled by DBRs in CRIGICs. In other words, it was found that the substrate radiation by DBRs in CRIGIC would degrade the performance of the drop demultiplexer seriously, and should be avoided in practical applications. One way to reduce the radiation loss can be a mode profile shifting by waveguide-structure modification so that the electric field of TE_0 mode at CRIGIC layer is too small to be diffracted. For example, as is

#132794 - $15.00 USD Received 2 Aug 2010; revised 2 Nov 2010; accepted 5 Nov 2010; published 17 Nov 2010

described in [18], we can design a double-core structure consisting of a higher-refractive-index main-guiding core underneath a sub-guiding core so that TE_0 mode is mainly confined in the main-guiding core without the electric field at the CRIGIC layer on the sub-guiding core. Another way may be a changing the role of TE_0 and TE_1 modes so that the grating vector of DBR in CRIGIC is designed to couple two contra-directional TE_0 input/output waves and is too large to diffract TE_1 signal-transmission wave. The changing of the role can be easily realized by modifying grating periods and lengths of CRIGICs for TE_0 mode, though the crosstalk noise level will slightly increase in the present structure.

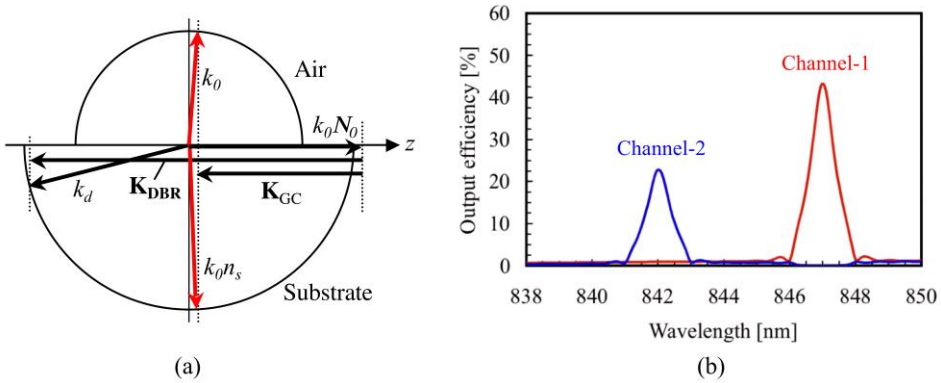

Fig. 7. (a) Wave vector diagram of CRIGIC that couples with TE_0 mode. (b) Calculated wavelength dependence of tow-channel demultiplexer using CRIGICs with consideration for the substrate radiations by DBRs in CRIGICs.

5. Conclusions

We have designed and fabricated a prototype free-space-wave drop demultiplexer by integration of CRIGICs and DGM-DBRs for the first time. The designed device with smaller aperture and simpler structure than those of the previously reported devices using GCs was investigated theoretically and experimentally. Two-channel drop demultiplexing from a guided wave to free-space waves was experimentally confirmed with the predicted great improvement in crosstalk noise reduction. An unpredicted and undesirable diffraction by DBRs in CRIGIC was observed experimentally. The reason for the diffraction was discussed theoretically, and two possible ways were proposed to eliminate such the unwanted diffraction. This will be one of key issues to construct ADMs for practical applications. The modification of the waveguide structure is currently under study in order to improve the device characteristics. Moreover, the application of the proposed ADMs to channel waveguides is also being investigated for practical optical interconnects.

#132794 - $15.00 USD Received 2 Aug 2010; revised 2 Nov 2010; accepted 5 Nov 2010; published 17 Nov 2010